Inorganic Chemistry

Article

pubs.acs.org/IC

Employment of a New Tripodal Ligand for the Synthesis of Cobalt(II/III), Nickel(II), and Copper(II) Clusters: Magnetic, Optical, and Thermal Properties

Angelos B. Canaj,[†] Demetrios I. Tzimopoulos,[‡] Aggelos Philippidis,[§] George E. Kostakis,[⊥] and Constantinos J. Milios*[,†]

[†]Department of Chemistry, The University of Crete, Voutes, 71003 Herakleion, Greece

[‡]Department of Chemistry, Aristotle University of Thessaloniki, 54124 Thessaloniki, Greece

[§]Institute of Electronic Structure and Laser, Foundation for Research and Technology-Hellas (IESL-FORTH), P.O. Box 1385, Crete, 71110 Herakleion, Greece

[⊥]Institute of Nanotechnology, Karlsruhe Institute of Technology, Hermann-von-Helmholtz Platz 1, 76344 Eggenstein-Leopoldshafen, Germany

Supporting Information

ABSTRACT: The employment of 2-(β-naphthalideneamino)-2-(hydroxymethyl)-1-propanol (LH_3) in cobalt, nickel, and copper chemistry has led to the isolation of five new metallic complexes with interesting magnetic properties. More specifically, the reaction of $Co(OAc)_2{\cdot}4H_2O$ with LH_3 in MeOH in the presence of NEt_3 under solvothermal conditions forms the complex $[Co^{III}_2Co^{II}_3(L)_2(LH)_2(L')(OAc)]{\cdot}8.5MeOH$ (**1**·8.5MeOH; L′ = monoanion of 2-hydroxy-1-naphthaldehyde), while in nickel chemistry, a similar reaction of $Ni(OAc)_2{\cdot}6H_2O$ with LH_3 in MeCN in the presence of NEt_3 under high pressure/temperature forms the complex $[Ni^{II}(LH_2)_2]{\cdot}2MeCN$ (**2**·2MeCN). Repeating the same reaction in MeOH and switching from $Ni(OAc)_2{\cdot}4H_2O$ to $NiSO_4{\cdot}4H_2O$ produces the complex $[Ni^{II}_4(HL)_3(OMe)(MeOH)_3](SO_4)_{0.5}{\cdot}2MeOH$ (**3**·2MeOH) under solvothermal conditions. Furthermore, in copper chemistry, the reaction of $Cu_2(OAc)_4{\cdot}2H_2O$ with LH_3 in the presence of NEt_3 in MeOH under solvothermal conditions affords the complex $[Cu^{II}_4(LH)_4]$ (**4**), while the same reaction under ambient temperature and pressure conditions forms $[Cu^{II}_4(LH)_4]{\cdot}3.5MeOH{\cdot}2.25H_2O$ (**5**·3.5MeOH·2.25H_2O). Complex **1** is a mixed-valent $[Co^{III}_2Co^{II}_3]$ complex, consisting of three edge-sharing $[Co_3]$ triangles. Complex **2** is a nickel(II) monomer in which the central metal is found in an octahedral geometry, while complex **3** describes a $[Ni^{II}_4]$ cubane. Complexes **4** and **5** may be considered as structural isomers because they possess the same formulas but different topologies: **4** describes a highly distorted $[Cu^{II}_4(OR)_4]^{4+}$ eight-membered ring, while **5** consists of a distorted $[Cu^{II}_4(\mu_3\text{-}OR)_4]^{4+}$ cubane. In addition, **5** can be converted to **4** in excellent yield under solvothermal conditions. Direct-current magnetic susceptibility studies have been carried out in the 5−300 K range for complexes **1** and **3**−**5**, revealing the possibility of a high-spin ground state for **1**, an $S = 4$ ground state for **2**, and diamagnetic ground states for **4** and **5**.

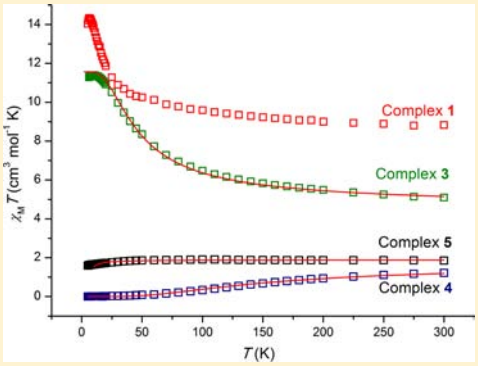

INTRODUCTION

The synthesis of metallic cluster compounds has advanced greatly in recent years because of the potential that such compounds display for new technological applications.[1] For example, in the field of *Magnetic Refrigeration*, metallic clusters with large magnetic spin ground states, *S*, are used to lower the temperature of their surroundings, as dictated by the magnetocaloric effect,[2] and molecules are now able to retain their magnetization above liquid-helium temperature once magnetized.[3] In the field of catalysis, oligonuclear and polynuclear complexes display excellent catalytic functionalities, and sustained water oxidation photocatalysis by a bioinspired manganese cluster is now plausible.[4] Finally, lanthanide-based clusters find applications in optics as lasers and light-emitting diodes, optical fibers, amplifiers, and near-IR-emitting materials.[5]

We recently initiated a project toward the synthesis and characterization of hybrid molecular species, i.e., molecules that display two different physical properties, because such materials would be at the interface of various scientific fields. More specifically, we are interested in synthesizing complexes that display both magnetic and optical/photoluminescent properties.[6] In order to construct such hybrid species, one may follow two main synthetic approaches: (i) start with molecules already possessing one of the two desired properties and attempt to

Received: August 8, 2012
Published: September 18, 2012

dx.doi.org/10.1021/ic301744e | *Inorg. Chem.* 2012, 51, 10461−10470

Scheme 1. Structure of LH_3 and Its Coordination Modes in 1−5

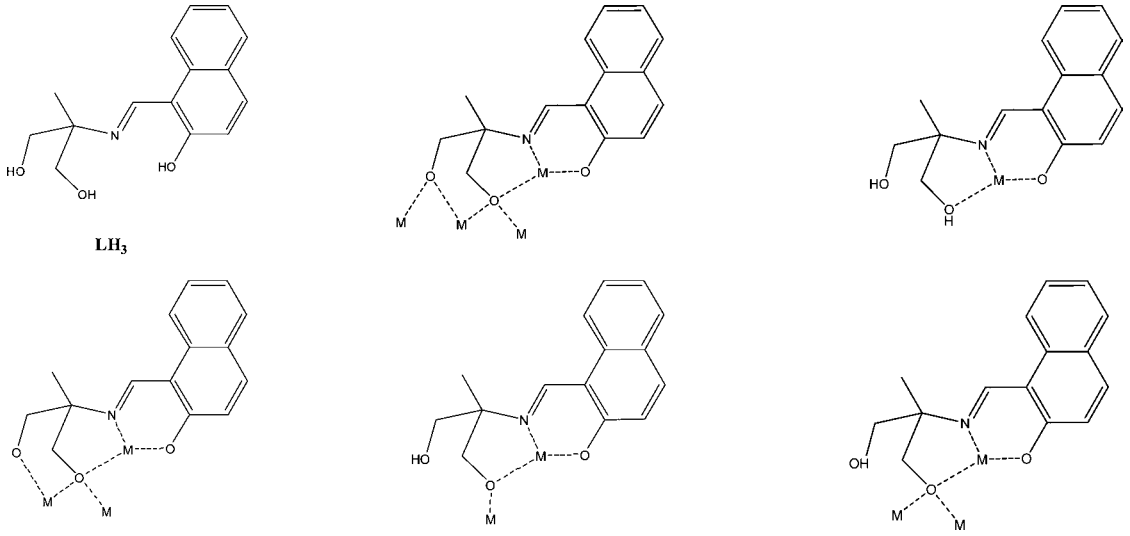

Table 1. Crystallographic Data for Complexes 1−5

	1·8.5MeOH	2·2MeCN	3·2MeOH	4	5·3.5MeOH·2.25H_2O
formula[a]	$C_{81.50}H_{102}Co_5N_4$ $O_{24.50}$	$C_{34}H_{38}N_4NiO_6$	$C_{102}H_{136}N_6Ni_8O_{34}S$	$C_{60}H_{60}Cu_4N_4O_{12}$	$C_{63.50}H_{78.50}Cu_4N_4O_{17.75}$
M_w	1824.32	657.39	2491.91	1283.28	1435.96
cryst syst	monoclinic	triclinic	monoclinic	monoclinic	monoclinic
space group	$P2_1/n$	$P\bar{1}$	$C2/c$	$C2/c$	$P2_1/c$
a/Å	16.093(2)	8.7371(17)	19.5108(11)	19.720(2)	19.808(9)
b/Å	18.4290(14)	13.993(2)	24.3167(12)	14.6735(17)	26.728(9)
c/Å	29.824(4)	15.172(3)	23.3917(11)	18.5807(17)	13.601(7)
α/deg		110.521(13)			
β/deg	91.442(11)	103.869(15)	104.115	93.943(8)	93.89(4)
γ/deg		103.934(14)			
V/Å^3	8842.1(17)	1575.3(5)	10762.8(10)	5363.7(10)	7184(5)
Z	4	2	4	4	4
T/K	180	180	180	180	180
λ[b]/Å	0.71073	0.71073	0.71073	0.71073	0.71073
D_c/g cm^{-3}	1.370	1.386	1.538	1.589	1.328
μ(Mo Ka)/mm^{-1}	0.99	0.67	1.47	1.63	1.23
measd/indep (R_{int}) refl.	41941/15644 (0.117)	9682/5891 (0.044)	32038/10102 (0.026)	9755/4951 (0.123)	61516/13579 (0.201)
obsd reflns [$I > 2\sigma(I)$]	6434	3624	7633	2472	5209
wR2[b,c]	0.188	0.081	0.067	0.157	0.219
R1[c,d]	0.085	0.044	0.031	0.069	0.081
GOF on F^2	1.010	0.953	1.046	0.949	1.004
$\Delta\rho_{max}$, $\Delta\rho_{min}$/e Å^{-3}	0.62, −0.34	1.19, −0.30	0.55, −0.41	0.47, −0.69	1.22, −0.57

[a]Including solvate molecules, Mo Kα radiation, graphite monochromator. [b]wR2 = $[\sum w|F_o^2| - |F_c^2|)^2/\sum w|F_o^2|^2]^{1/2}$. [c]For observed data. [d]R1 = $\sum||F_o| - |F_c||/\sum|F_o|$.

incorporate the second property[7] or (ii) simply mix the "carriers" of the two properties in the presence of a suitable linker following the principles of serendipitous self-assembly.[8] In this work, we present the results obtained upon employment of the emissive ligand 2-(β-naphthalideneamino)-2-(hydroxymethyl)-1-propanol (LH_3; Scheme 1) in cobalt, nickel, and copper chemistry, as well as the magnetic, optical, and thermal properties of the clusters isolated. This ligand was previously employed by our group in dysprosium(III) chemistry, leading to a bright-blue-emissive [Dy^{III}_7] single-molecule magnet.[9]

EXPERIMENTAL SECTION

All manipulations were performed under aerobic conditions, using materials as received. LH_3 was synthesized by the reaction of 2-hydroxy-1-naphthaldehyde with 2-amino-2-methyl-1,3-propanediol in MeOH, as described in the literature.[10]

[$Co^{III}_2Co^{II}_3$(L)$_2$(LH)$_2$(L′)(OAc)]·8.5MeOH (1·8.5MeOH). Co(OAc)$_2$·4H_2O (125 mg, 0.5 mmol), LH_3 (130 mg, 0.5 mmol), and NEt_3 (3.0 mmol) were added in MeOH (10 mL), and the resulting mixture was transferred to a Teflon-lined autoclave and kept at 120 °C for 12 h. After slow cooling to room temperature, red-brown crystals of [$Co^{III}_2Co^{II}_3$(L)$_2$(LH)$_2$(L′)(OAc)]·8.5MeOH were obtained in ∼30% yield, collected by filtration, washed with Et_2O, and dried in air. The complex analyzed as **1**·2MeOH. Anal. Calcd for $C_{75}H_{78}Co_5N_4O_{18}$: C, 55.67; H, 4.86; N, 3.46. Found: C, 55.84; H, 5.03; N, 3.24.

[Ni^{II}(LH$_2$)$_2$]·2MeCN (2·2MeCN). Ni(OAc)$_2$·4H_2O (249 mg, 1 mmol), LH_3 (259 mg, 1.0 mmol), and NEt_3 (2.0 mmol) were added in MeCN (10 mL), and the resulting mixture was transferred to a Teflon-lined autoclave and kept at 120 °C for 12 h. After slow cooling to

dx.doi.org/10.1021/ic301744e | Inorg. Chem. 2012, 51, 10461−10470

room temperature, dark-yellow crystals of $[Ni^{II}(LH_2)_2]\cdot 2MeCN$ were obtained in ~30% yield, collected by filtration, washed with Et_2O, and dried in air. Anal. Calcd for $C_{30}H_{32}NiN_2O_6$: C, 62.63; H, 5.61; N, 4.87. Found: C, 62.49; H, 5.37; N, 4.61.

$[Ni^{II}_4(HL)_3(OMe)(MeOH)_3](SO_4)_{0.5}\cdot 2MeOH$ (3·2MeOH). $NiSO_4\cdot 6H_2O$ (372 mg, 1 mmol), LH_3 (259 mg, 1.0 mmol), and NEt_3 (3.0 mmol) were added in MeOH (10 mL), and the resulting mixture was transferred to a Teflon-lined autoclave and kept at 120 °C for 12 h. After slow cooling to room temperature, dark-yellow crystals of $[Ni^{II}_4(HL)_3(OMe)(MeOH)_3](SO_4)_{0.5}\cdot 2MeOH$ were obtained in ~45% yield, collected by filtration, washed with Et_2O, and dried in air. The complex analyzed as solvent-free. Anal. Calcd for $C_{98}H_{120}Ni_8N_6O_{30}S$: C, 49.80; H, 5.12; N, 3.56. Found: C, 49.67; H, 4.89; N, 3.68.

$[Cu^{II}_4(LH)_4]$ (4). $Cu_2(OAc)_4\cdot 2H_2O$ (200 mg, 0.5 mmol), LH_3 (259 mg, 1.0 mmol), and NEt_3 (3.0 mmol) were added in MeOH (10 mL), and the resulting mixture was transferred to a Teflon-lined autoclave and kept at 120 °C for 12 h. After slow cooling to room temperature, dark-blue crystals of $[Cu^{II}_4(LH)_4]$ were obtained in ~40% yield, collected by filtration, washed with Et_2O, and dried in air. Anal. Calcd for $C_{60}H_{60}Cu_4N_4O_{12}$: C, 56.16; H, 4.71; N, 4.37. Found: C, 56.28; H, 4.45; N, 4.25.

$[Cu^{II}_4(LH)_4]\cdot 3.5MeOH\cdot 2.25H_2O$ (5·3.5MeOH·2.25H$_2$O). $Cu_2(OAc)_4\cdot 2H_2O$ (200 mg, 0.5 mmol), LH_3 (259 mg, 1.0 mmol), and NEt_3 (3.0 mmol) were added in MeOH (10 mL), and the resulting mixture was stirred for ~1 h. The solution was filtered and allowed to evaporate at room temperature. After 2 days, dark-blue crystals of $[Cu^{II}_4(LH)_4]\cdot 3.5MeOH\cdot 2.25H_2O$ were obtained in ~40% yield, collected by filtration, washed with Et_2O, and dried in air. The sample was analyzed as $5\cdot 2MeOH\cdot H_2O$ Anal. Calcd for $C_{62}H_{70}Cu_4N_4O_{15}$: C, 54.54; H, 5.17; N, 4.10. Found: C, 54.67; H, 5.43; N, 3.96.

Physical Methods. Elemental analyses (C, H, and N) were performed by the University of Ioannina microanalysis service. Variable-temperature, solid-state direct-current (dc) magnetic susceptibility data down to 2.0 K were collected on a Quantum Design MPMS-XL SQUID magnetometer equipped with a 7 T dc magnet at The University of Crete. Diamagnetic corrections were applied to the observed paramagnetic susceptibilities using Pascal's constants.

X-ray Crystallography and Structure Solution. Data collection parameters and structure solution and refinement details are listed in Table 1. Full details for **1**–**3** can be found in the CIF files provided in the Supporting Information. Full details for **4** and **5** can be found in the CIF files with CCDC 885411 and 885412, respectively. The atomic coordinates for these structures have been deposited with the Cambridge Crystallographic Data Centre. The coordinates can be obtained, upon request, from the Director, Cambridge Crystallographic Data Centre, 12 Union Road, Cambridge CB2 1EZ, U.K.

RESULTS AND DISCUSSION

Synthesis. The reaction between $Co(OAc)_2\cdot 4H_2O$ and LH_3 in the presence of base (NEt_3) in MeOH under solvothermal conditions gives the pentanuclear mixed-valent cluster **1**·8.5MeOH in good yield. The identity of the compound was a surprise for us for three reasons: (i) almost half of the cobalt atoms were found in the 3+ oxidation state, despite the fact that the starting material contained exclusively cobalt(II) and that the experiment was performed under mild reducing conditions (high temperature and high pressure), (ii) a part of the ligand employed was transformed to the monoanion of 2-hydroxy-1-naphthaldehyde, and (iii) despite the excess of base used in the reaction, an amount of the ligand employed was not fully deprotonated. Therefore, we investigated all of the parameters of the above synthetic scheme, e.g., the amount and nature of the base employed and the temperature/time of the reaction, but all of our attempts led to the same product, as established by means of powder X-ray diffraction (PXRD). In order to investigate whether the pentanuclear cluster is formed only under solvothermal conditions, we repeated the same reaction under normal bench conditions, but we only managed to isolate a pink precipitate of unknown identity and different PXRD to that of **1**, indicating that indeed complex **1** forms only under high temperature/pressure.

Given the similarity of nickel and cobalt chemistry, we thought of employing LH_3 in nickel chemistry as a means of obtaining analogous nickel(II) clusters. The reaction between $Ni(OAc)_2\cdot 4H_2O$ and LH_3 in the presence of base (NEt_3) in MeCN under solvothermal conditions gives the mononuclear complex $[Ni^{II}(LH_2)_2]$, which was crystallographically identified as **2**·2MeCN, according to eq1.

$$Ni(OAc)_2\cdot 4H_2O + 2LH_3 \xrightarrow{MeCN} [Ni^{II}(LH_2)_2] + 2OAcH + 4H_2O \quad (1)$$

Again, even though an excess of base was used in the reaction, only the monoanionic form of the ligand, LH_2^-, was formed. Therefore, we repeated the reaction by increasing the amount of the base used, but we were not able to isolate a different product than **2**, as was evidenced by a IR and PXRD comparison. Changing the metal salt to $NiSO_4$ as a means of affecting the system's behavior and repeating the solvothermal reaction led to a green-white insoluble powder, which could not be identified. Then, by changing the solvent to MeOH and keeping all other parameters the same, we were able to isolate the tetranuclear complex **3**, which was crystallographically identified as **3**·2MeOH, according to eq2.

$$8NiSO_4 + 6LH_3 + 8MeOH \xrightarrow{MeOH} 2[Ni^{II}_4(LH)_3(OMe)(MeOH)_3](SO_4)_{0.5} + 7H_2SO_4 \quad (2)$$

Complex **3** is a tetranuclear $[Ni^{II}_4]$ cluster in which the ligand is found in its dianionic form, LH^{2-}. Furthermore, the metal-to-ligand ratio is 4:3 compared to 1:2 in complex **2**, even though in both preparations the same metal-to-ligand ratio of 1:1 was initially used, possibly indicating the role of the solvent in deprotonation of LH_3. Interestingly, for the formation of both **2** and **3**, the solvothermal conditions are no prerequisites because they also form under normal bench conditions in moderate yield.

Finally, in copper chemistry, the reaction between $Cu_2(OAc)_4\cdot 2H_2O$ and LH_3 in the presence of base (NEt_3) in MeOH under solvothermal conditions gives the tetranuclear complex **4**, according to eq3.

$$2Cu_2(OAc)_4\cdot 2H_2O + 4LH_3 \xrightarrow{MeOH} [Cu^{II}_4(LH)_4] + 8OAcH + 4H_2O \quad (3)$$

Repeating exactly the same reaction but under ambient temperature and pressure conditions yields dark-blue crystals of **5**·3.5MeOH·2.25H$_2$O in very good yield. Complexes **4** and **5** may be considered as structural isomers; that is, they possess the same formulas (excluding the cocrystallized solvent molecules) but different structures (vide infra), a "metallocyclic" structure for **4** versus the more "compact" cubane structure for **5**. More specifically, complex **4** can be thought of as a structural rearrangement during the "breaking" of complex **5**. Indeed, **5** can be transformed to complex **4** in excellent yield by simply heating it in MeOH under solvothermal conditions,

as confirmed by PXRD analysis (Figure 1). We also tried to convert **4** to **5** by different methods, using a large variety of

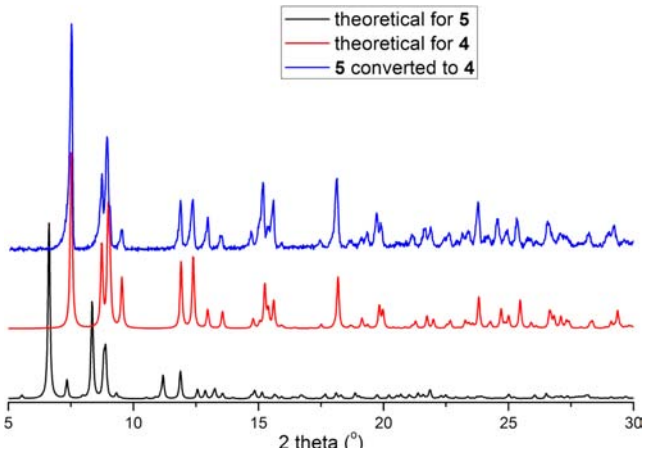

Figure 1. PXRD diagram comparison between complexes **4** and **5** and conversion of **5** to **4** under solvothermal conditions.

solvents and changing a lot of synthetic parameters, but all of our efforts were fruitless. Even though there are numerous [Cu^{II}_4] clusters reported in the literature (more than 1600 complexes in the CCDC) and the cubane topology is very common with more than 400 examples, there are only a handful of complexes presenting the eight-membered ring topology of **4**.[11]

Description of Structures. The structure of complex **1** is shown in Figure 2 with selected bond lengths and angles given in Table S1 in the Supporting Information. Complex **1** crystallizes in the monoclinic $P2_1/n$ space group. It consists of three edge-sharing [$Co_3(\mu_3\text{-}O_R)$] triangles, two of which are scalene (the peripheral ones) and one isosceles (the central one). Each peripheral triangle is held by one μ_3-O_R alkoxide group belonging to a doubly deprotonated $\eta^3{:}\eta^1{:}\eta^1{:}\eta^1{:}\mu_3$ LH^{2-} ligand and one μ_2-O_R alkoxide belonging to a fully deprotonated $\eta^3{:}\eta^2{:}\eta^1{:}\eta^1{:}\mu_3$ L^{3-} ligand. On the contrary, the central triangle is held in position by the four μ_3-O_R alkoxide groups belonging to the four ligands present in the structure. The dimensions of the peripheral triangles fall in the 2.86−3.81 Å range, while for the central triangle, the dimensions fall in the 2.86−3.04 Å range. All metal centers are six-coordinate, adopting slightly distorted octahedral geometries, while the coordination environment is completed by the presence of one acetate in bridging $\eta^1{:}\eta^1{:}\mu$ mode and one chelate, monianionic 2-hydroxy-1-naphthaldehyde. Charge considerations necessitate for the presence of three cobalt(II) and two cobalt(III), and based on bond distances, Co1 and Co5 are in the 3+ oxidation state (all bond distances are in the 1.8−1.9 Å range), while Co2, Co3, and Co4 are assigned to the 2+ oxidation state (bond distances in the 2.0−2.2 Å range). In the crystal lattice, the molecules of **1** pack in a "head-to-tail" fashion, forming dimers via four MeOH solvent molecules through hydrogen bonds (Figure 2, right).

Complex **2** crystallizes in the triclinic space group $P\bar{1}$ (Figure 3 and Table S2 in the Supporting Information). The central

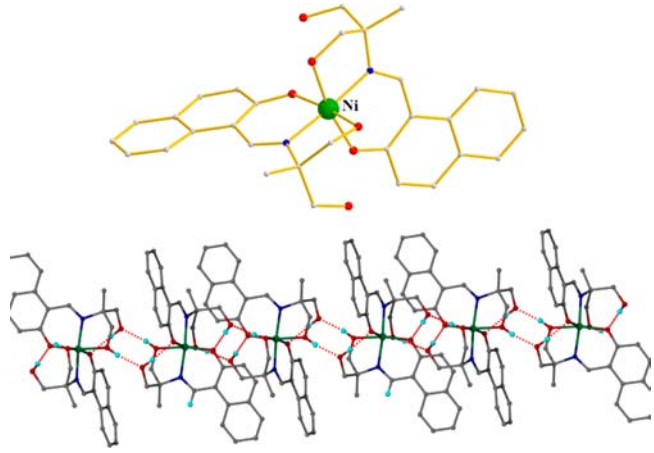

Figure 3. Molecular structure of complex **2** (top). Hydrogen-bond "zig-zag" formation in **2** (bottom). Color code: Ni^{II}, green; O, red; N, blue; C, gray.

Ni^{II} atom is tightly bound with two mononionic LH_2^- ligands, through two six-membered and two five-membered chelate rings. The coordination sphere of the Ni^{II} atom is O_4N_2, with the complex adopting the trans conformation. In the lattice, the complex forms hydrogen bonds through the nondeprotonated −OH groups of the LH_2^- ligands, linking neighboring complexes in a "tape" fashion (Figure 3, bottom). Each cluster

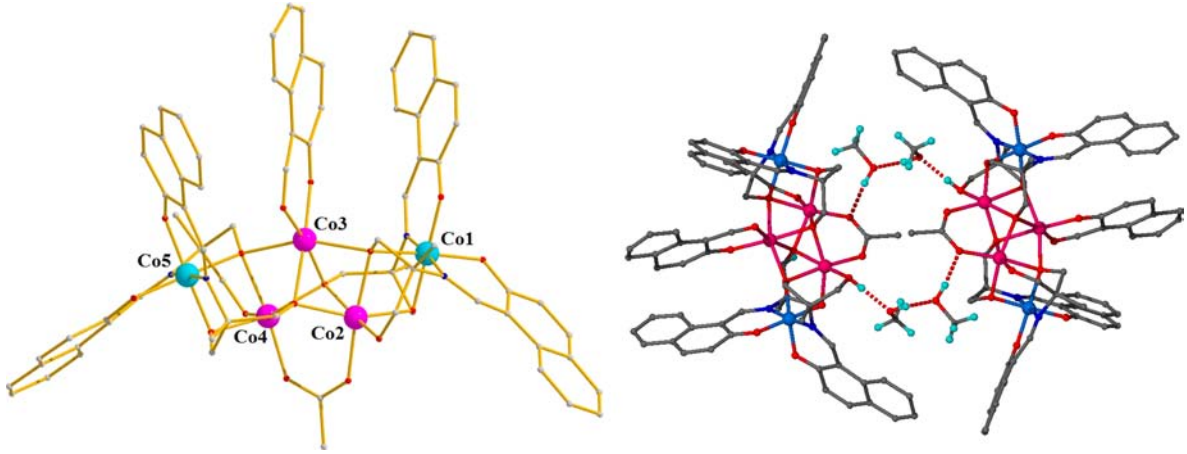

Figure 2. Molecular structure of complex **1** (left). Hydrogen-bond formation in **1** (right). Color code: Co^{II}, pink; Co^{III}, pale blue; O, red; N, blue; C, gray.

dx.doi.org/10.1021/ic301744e | Inorg. Chem. 2012, 51, 10461−10470

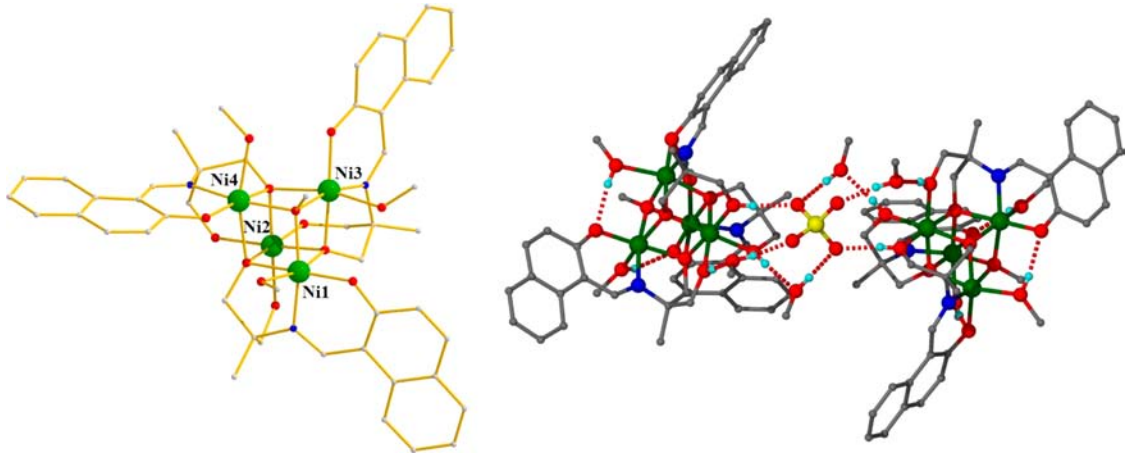

Figure 4. Molecular structure of the cationic part of complex **3** (left). Hydrogen-bond formation in **3** (right). Color code: Ni^{II}, green; O, red; N, blue; C, gray; S, yellow.

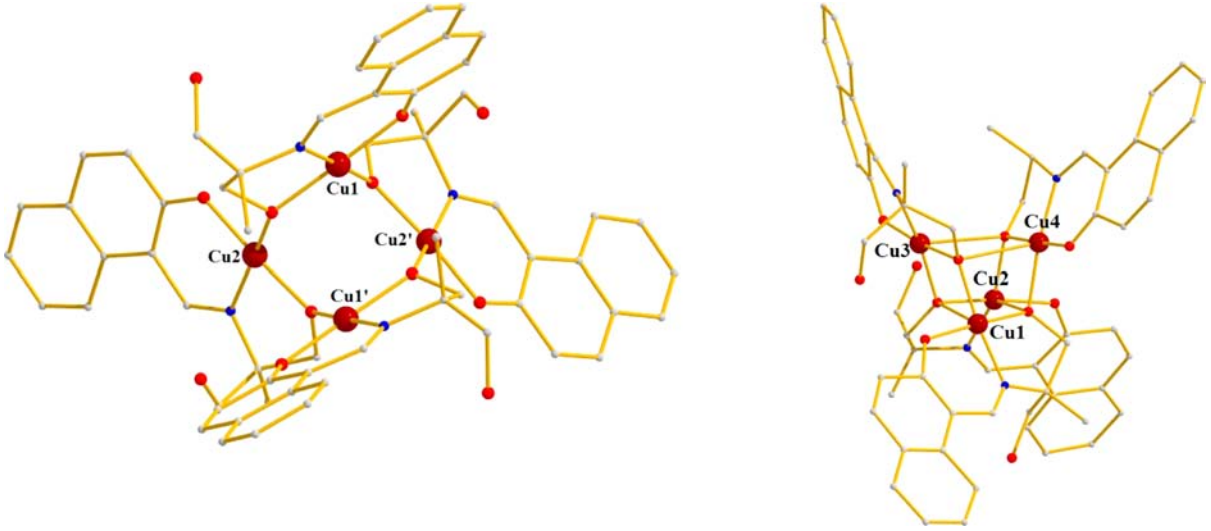

Figure 5. Molecular structures of complexes **4** (left) and **5** (right). Color code: Cu^{II}, brown; O, red; N, blue; C, gray.

forms four hydrogen bonds to two neighboring complexes, resulting in a "zig-zag" 1D arrangement of clusters.

Complex **3** crystallizes in the monoclinic space group *C*2/*c* (Figure 4 and Table S3 in the Supporting Information). Its core describes a $[Ni^{II}_4(OR)_4]^{4+}$ cubane, which is held by three doubly deprotonated ligands, LH^{2-}, and one methoxide group. The three dianionic ligands are found in a $\eta^3{:}\eta^1{:}\eta^1{:}\eta^1{:}\mu_3$ coordination mode, while the methoxide serves as a monatomic μ_3 bridge. Each Ni^{II} center is six-coordinated, adopting octahedral geometry, while the coordination environment is completed by the three MeOH molecules. Furthermore, the octahedral geometry for Ni1, Ni3, and Ni4 is axially distorted, as evidenced by the elongated axial bonds, which are ∼0.18 Å longer than the equatorial ones. In the crystal lattice, "dimers" of clusters are formed (Figure.4, right) with the aid of the SO_4^{2-} group, which serves as the "linker", forming four hydrogen bonds to two neighboring clusters and three MeOH solvate molecules. A detailed CCDC search according to the algorithm reported by Kostakis et al.[12] revealed the presence of 109 previously reported tetranuclear $[Ni^{II}_4]$ clusters adopting the cubane metal topology.

Complex **4** crystallizes in the monoclinic space group *C*2/*c* (Figure 5, left, and Table S4 in the Supporting Information). Its core describes a severely puckered $[Cu^{II}_4(OR)_4]^{4+}$ eight-membered ring of four square-planar four-coordinate Cu^{II} centers linked via four alkoxide groups from four doubly deprotonated LH^{2-} ligands; the latter are all found in the $\eta^2{:}\eta^1{:}\eta^1{:}\mu$ coordination mode. The distances between neighboring Cu^{II} ions are in the 3.40−3.45 Å range, while the distances between opposite Cu^{II} ions are 3.56 and 4.04 Å for Cu1−Cu1′ and Cu2−Cu2′, respectively. The Cu−O(R) distances are all in the 1.90−1.92 Å range. Finally, all Cu−O(R)−Cu angles are above 124°, while the puckering of the $[Cu^{II}_4(OR)_4]^{4+}$ ring is evidenced by the dihedral angle of ∼40° between the two $\{Cu_2(OR)_2\}$ subunits of the wheel. In the crystal lattice, complex **4** forms a "tape" through the *c* axis via the formation of four hydrogen bonds (Figure SI1 in the Supporting Information). Complex **5** (Figure 5, right, and Table S5 in the Supporting Information) crystallizes in the monoclinic space group $P2_1/c$. Its core consists of a distorted $[Cu^{II}_4(\mu_3\text{-}OR)_4]^{4+}$ cubane assembled by four $\eta^3{:}\eta^1{:}\eta^1{:}\mu_3$ doubly deprotonated LH^{2-} ligands. All Cu^{II} ions may be considered as displaying essentially square-planar geometry, with an additional weak axial interaction of ∼2.5−2.7 Å. The dimensions of the metallic tetrahedron are in the range of 3.116−3.533 Å, with the shortest distance for Cu2···Cu4 and

dx.doi.org/10.1021/ic301744e | *Inorg. Chem.* 2012, 51, 10461−10470

the longest for Cu1···Cu2. The two Cu2−(μ_3-O_R)−Cu4 angles are 87.8 and 107.2°, while the corresponding ones for Cu1−(μ_3-O_R)−Cu3 are 86.6 and 116.0°. Complex **5** in the crystal forms a complicated network of hydrogen bonding, leading to the formation of channels running through the *c* axis (Figure SI2 in the Supporting Information).

A careful look at the structures of complexes **4** and **5** reveals an interesting finding about the structures of **4** and **5**; more specifically, in complex **4**, there are long contacts for Cu1···O2 (3.05 Å), Cu2···O5 (3.19 Å), and their symmetry-related equivalents in the inorganic core, which when linked together, form the distorted cubane structure of **5** (Scheme 2).

Scheme 2. Core of 4 Assuming the Long Contacts (Dashed Lines) as Bonding Distances Yielding the Distorted Cubane Core of Complex 5

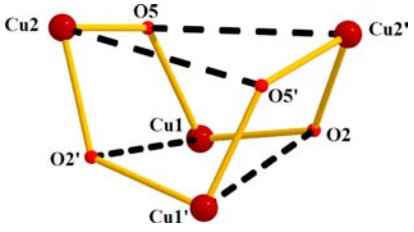

dc Magnetic Susceptibility Studies. dc magnetic susceptibility studies were performed on polycrystalline samples of complexes **1** and **3**−**5** in the 5−300 K range in an applied field of 0.1 T. The results are plotted as the $\chi_M T$ product versus *T* in Figures 6−8 for complexes **1**, **3**, and **4** and **5**, respectively.

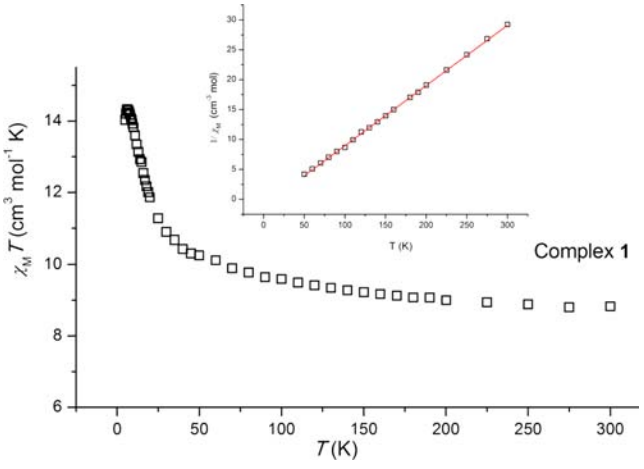

Figure 6. Plot of $\chi_M T$ versus *T* for complex **1**. Inset: Curie−Weiss plot for complex **1** in the 50−300 K range.

For complex **1**, the room temperature $\chi_M T$ value of 8.82 cm^3 K mol^{-1} corresponds to three noninteracting Co^{II} ions with $S = {}^3/_2$ and $g = 2.50$. Upon cooling, the $\chi_M T$ value increases to a maximum value of 14.32 cm^3 K mol^{-1} at 6.5 K, below which it slightly drops to a minimum value of 14.16 cm^3 K mol^{-1} at 5 K. Given the presence of octahedral Co^{II} ions with a $^4T_{1g}$ ground-state term, which splits to a doublet ground state at low temperature when in a distorted environment because of spin−orbit coupling,[13] it is very laborious and extremely difficult to apply an exact theoretical model for fitting the magnetic susceptibility data.[14] For instance, the low-temperature $\chi_M T$ value may be attributed to an $S = {}^9/_2$ ground state, assuming a *g*

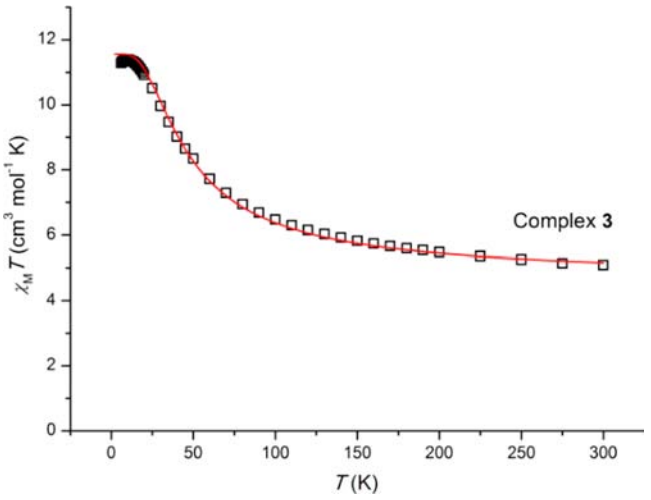

Figure 7. Plot of $\chi_M T$ versus *T* for **3**. The solid line represents a simulation of the data in the temperature range 5−300 K (see the text for details).

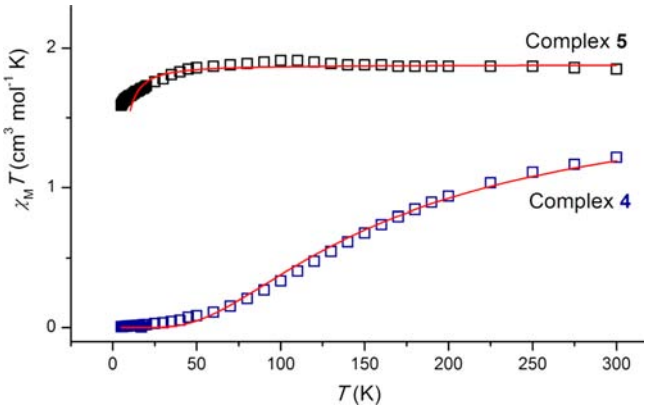

Figure 8. Plot of $\chi_M T$ versus *T* for complexes **4** (blue squares) and **5** (black squares). The solid line represents a simulation of the data in the temperature range 5−300 K (see the text for details).

value of 2.15. Yet, this is a very risky statement because Co^{II} is highly anisotropic and the magnetic exchange interactions in such systems are mainly dictated by the orientation of the local magnetic moments.[15] Furthermore, Co^{II} ions, when in octahedral geometry, may be treated as pseudo "$S_{eff} = 1/2$" systems at low temperature because of the splitting of the Kramers doublets. In order to have a qualitative view of the dominant interactions present in the system, we performed a Curie−Weiss analysis of the high-temperature (50−300 K) magnetic susceptibility data with $\theta = +11$ K (Figure 6, inset).

For complex **3**, the $\chi_M T$ value of 5.03 cm^3 K mol^{-1} at 300 K is very close to the spin-only ($g = 2.17$) value of 4.66 cm^3 K mol^{-1} expected for four high-spin Ni^{2+} ions. Upon cooling, this value starts to increase to a maximum value of 11.39 cm^3 K mol^{-1} at 9 K and then decreases slightly to 11.28 cm^3 K mol^{-1} at 5 K. This behavior is consistent with dominant ferromagnetic interactions within the metallic cluster, with the low-temperature $\chi_M T$ value suggesting a $S = 4$ ground state. The small drop of the $\chi_M T$ value below 9 K may be attributed to zero-field splitting and/or intermolecular interactions. Using the program *MAGPACK*,[16] we were able to successfully simulate the data assuming a 1*J* model, and employing the spin Hamiltonian in eq 4 allowed us to satisfactorily fit the data with the parameters

dx.doi.org/10.1021/ic301744e | *Inorg. Chem.* 2012, 51, 10461−10470

J = +5.7 cm^{-1} and g = 2.16. The ground state of the complex was found to be S = 4, with the first excited state of S = 3 located at 44 cm^{-1} above.

$$\hat{H} = -2J(\hat{S}_1\cdot\hat{S}_2 + \hat{S}_1\cdot\hat{S}_3 + \hat{S}_1\cdot\hat{S}_4 + \hat{S}_2\cdot\hat{S}_3 + \hat{S}_2\cdot\hat{S}_4 + \hat{S}_3\cdot\hat{S}_4) \quad (4)$$

The ferromagnetic nature of **3** is not uncommon for a [Ni$^{II}_4$] cubane because so far many similar examples have been reported.[17] Given that (i) the nature of the magnetic exchange interaction within a [Ni$^{II}_4$] cubane cluster is strongly dependent on the Ni−O−Ni angle and (ii) for Ni−O−Ni angles above ∼99° antiferromagnetic interactions are favored, while for Ni−O−Ni angles below ∼99° ferromagnetic interactions are established,[18] it is not surprising to find the ferromagnetic interaction in **3** because all Ni−O−Ni angles are lower than 99°.

For **4** and **5**, the $\chi_M T$ values at room temperature are 1.21 and 1.83 cm^3 K mol^{-1}, respectively, with only the value of **5** being very close to the expected value for four noninteracting (g = 2.20) Cu^{II} ions of 1.85 cm^3 K mol^{-1}. Upon cooling, the $\chi_M T$ value of **4** rapidly decreases, indicating the presence of strong antiferromagnetic interactions even at room temperature, reaching zero at ∼40 K. On the contrary, upon cooling, the $\chi_M T$ value of **5** slightly increases to a maximum value of 1.91 cm^3 K mol^{-1} at ∼60 K, below which it starts to decrease and reaches the minimum value of 1.59 cm^3 K mol^{-1} at 5 K. For **4**, we were able to successfully simulate the data assuming a 1J model, and employing the Hamiltonian in eq 5 allowed us to satisfactorily fit the data with the parameters J = −74.7 cm^{-1} and g = 2.20. The ground state of the complex was found to be S = 0, well-isolated from the first excited state of S = 1 located ∼150 cm^{-1} higher in energy.

$$\hat{H} = -2J(\hat{S}_1\cdot\hat{S}_2 + \hat{S}_2\cdot\hat{S}_3 + \hat{S}_3\cdot\hat{S}_4 + \hat{S}_1\cdot\hat{S}_4) \quad (5)$$

The magnitude and sign of the magnetic exchange interaction are due to the large Cu−O(R)−Cu angles (>125°) and Cu−O(R) distances present in **4** and are in good agreement with previously reported values in similar monobridged via an alkoxide/hydroxide group copper complexes.[19]

For **5**, we managed to simulate the data adopting a 2J model assuming the tetranuclear complex as a "dimer-of-dimers" (Figure 9).[20] According to this model, there are two different

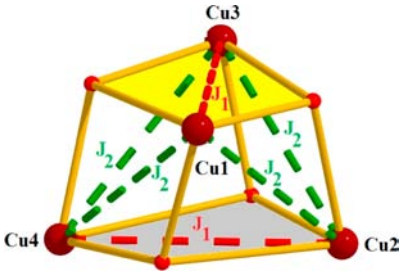

Figure 9. J-interaction scheme employed for **5** highlighting the two dimers present in the structure (in gray and yellow).

magnetic interactions: one intradimer (most commonly antiferromagnetic) interaction J_1, following a Hatfield and Hodgson type correlation, and an interdimer (usually weakly ferromagnetic) interaction depending only on the Cu···O distance or the angle between the two dimeric Cu_2O_2 planes but not on the Cu−O(R)−Cu angle. Using *MAGPACK* and the interaction scheme shown in Figure 9 and employing the Hamiltonian of eq 6, we managed to successfully simulate the data with the parameters J_1 = −3.2 cm^{-1}, J_2 = +1.1 cm^{-1}, and g = 2.23. The ground state of the complex was found to be S = 0, with the first excited state of S = 1 located at ∼6 cm^{-1} above.

$$\hat{H} = -2J_1(\hat{S}_1\cdot\hat{S}_3 + \hat{S}_2\cdot\hat{S}_4) - 2J_2(\hat{S}_1\cdot\hat{S}_4 + \hat{S}_1\cdot\hat{S}_2 + \hat{S}_3\cdot\hat{S}_4 + \hat{S}_2\cdot\hat{S}_3) \quad (6)$$

In an attempt to further determine the ground state of complex **3**, variable-temperature and variable-field dc magnetization data were collected in the ranges 2−7 K and 1−7 T. The magnetization data are plotted as reduced magnetization ($M/N\mu_B$) versus H/T in Figure 10. We were able to fit the 2−7

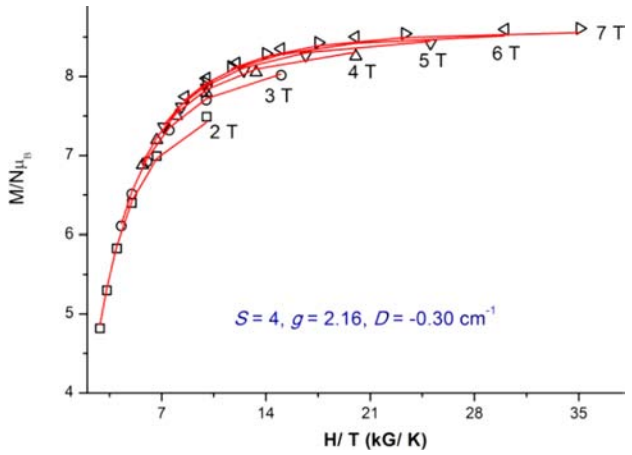

Figure 10. Plot of reduced magnetization ($M/N\mu_B$) versus H/T for **3** in 2−7 T fields and 2−7 K temperature range.

T field data, employing a matrix diagonalization method to a model that assumes only the ground state is populated, includes axial zero-field splitting ($D\hat{S}z^2$) and the Zeeman interaction, and carries out a full powder average. The corresponding Hamiltonian is given by eq7

$$\hat{H} = D\hat{S}z^2 + g\mu_B\mu_0\hat{S}\cdot H \quad (7)$$

where D is the axial anisotropy, μ_B is the Bohr magneton, μ_0 is the vacuum permeability, $\hat{S}z$ is the easy-axis spin operator, and H is the applied field. The best fit gave S = 4, g = 2.16 (in excellent agreement with the magnetic susceptibility simulation parameters), and D = −0.30 cm^{-1}.

Thermal Decomposition Properties. Thermogravimetric analyses (TG/DTG) were carried out on polycrystalline samples of **1**·8.5MeOH, **3**·2MeOH, **4**, and **5**· 3.5MeOH·2.25-H_2O in the 40−400 °C temperature range (Figure 11). The thermal decomposition of complex **1**·8.5MeOH starts with a weight loss of ∼12% in the 40−240 °C region, corresponding to the loss of 8.5 mol of MeOH per 1 mol of complex **1**·8.5MeOH (theoretical loss of 14%), with the desolvated product being thermally unstable because no plateau is observed. The cluster continues to decompose, displaying two weight losses of ∼9.5% and 27% in the 242−335 and 350−415 °C temperature ranges, respectively, corresponding to the loss of the L′H fragment (theoretical loss of 9.54%) and two LH_3 species (theoretical value of 28.4%), respectively. Complex **3**·2MeOH starts with a weight loss of ∼12% in the 40−130 °C region, corresponding to the loss of 5 mol of MeOH per 1 mol of complex **3**·2MeOH (theoretical loss of 12.8%), two of which are the cocrystallized ones and the remaining three the

dx.doi.org/10.1021/ic301744e | Inorg. Chem. 2012, 51, 10461−10470

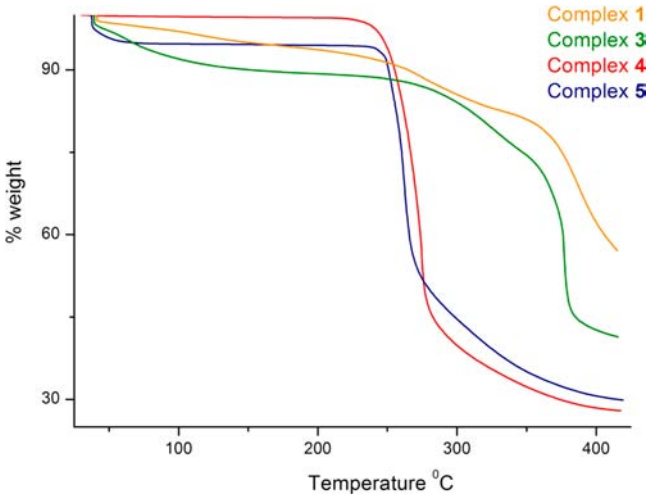

Figure 11. TG/DTG of complexes **1**·8.5MeOH, **3**·2MeOH, **4**, and **5**·**5**·3.5MeOH.2.25H_2O, in the 40−400 °C temperature range.

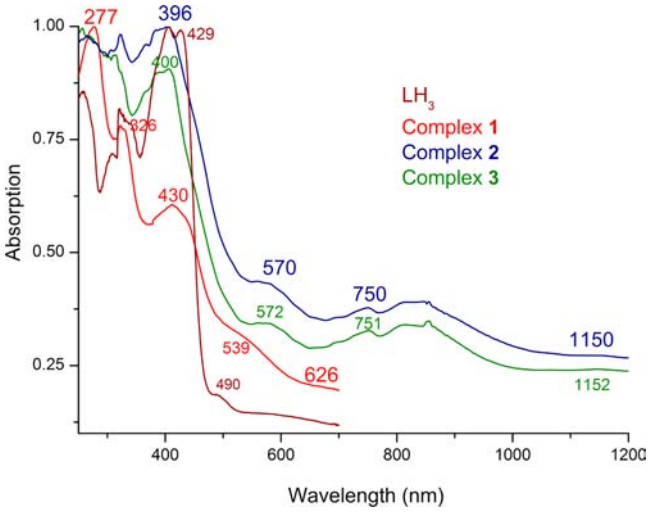

Figure 12. Solid-state UV−vis spectra (normalized) for complexes **1**−**3** and LH_3.

terminally coordinated ones, with the desolvated product being thermally stable because a plateau is observed in the 130−240 °C temperature range. Above this temperature, the product decomposes rapidly in the 240−393 °C temperature range in a two-step process of a total ∼45% weight loss corresponding to the loss of two LH_3 ligands and a half sulfate molecule (theoretical loss of 45.2%).

Complex **4** shows no weight loss in the early temperature range 40−80 °C, in good agreement with the absence of solvent molecules. The complex remains stable until ∼221 °C, above which it starts to dissociate. On the contrary, complex **5** starts with a weight loss of ∼7.5% in the 40−80 °C region, corresponding to the loss of 3.5 mol of CH_3OH and 2.25 mol of H_2O per 1 mol of complex **5**·3.5MeOH·2.25H_2O (theoretical loss of 10.6%). The deviation between the experimentally observed and theoretical loss values should be attributed to the loss of MeOH solvent molecules (∼1.5 mol of MeOH per 1 mol of complex **5**·3.5MeOH·2.25H_2O) while standing on air before the start of the measurement. In the 90−238 °C temperature range, the plateau indicates a thermally stable product that decomposes rapidly above 238 °C. Comparing the two complexes, we observe that both of them display the same pattern above ∼80 °C (i.e., when **5** loses its solvent molecules), and by comparing the thermal dissociation points, we see that the "compact" cubane structure displays higher thermal stability than the wheel because it starts to decompose at higher temperature (238 vs 221 °C for **4**). This is in good agreement with the conversion of **5** to **4** under solvothermal conditions because energy is required in order to "force" the more stable complex **5** to form **4**.

Optical Properties. The solid-state electronic absorption spectra of complexes **1**−**3** are shown in Figure 12. For **1**, the peak at ∼430 nm, as well as the shoulders at 539 and 625 nm, may be attributed to octahedral Co^{II} ions and more specifically to the $^4T_{1g} \rightarrow {}^4T_{1g}(P)$ and $^4T_{1g} \rightarrow {}^4A_{2g}$ transitions, respectively.[21] This complicated structure is due to spin−orbit coupling effects and an admixture of spin-forbidden transitions to doublet states. Complexes **2** and **3** display similar spectra with small differences because of the different coordination environments of the Ni ions in the complexes; in **2**, there is only one coordination sphere for the Ni^{II} ion (O_4N_2), while for **3**, Ni^{II} ions adopt two different coordination environments, O_5N for Ni1, Ni3, and Ni4 and O_6 for Ni2. The solid-state electronic spectrum of the compounds can be assigned to d−d transitions in octahedral geometry. Assuming O_h symmetry, the bands at 396 (25250 cm^{-1}), 750 (shoulder) (13335 cm^{-1}), and 1150 nm (8695 cm^{-1}) are assigned to the three spin-allowed transitions $^3A_{2g} \rightarrow {}^3T_{1g}(P)$, $^3A_{2g} \rightarrow {}^3T_{1g}(F)$, and $^3A_{2g} \rightarrow {}^3T_{2g}$ respectively. The shoulder at 570 nm (17545 cm^{-1}) is tentatively assigned to the spin-forbidden $^3A_{2g} \rightarrow {}^1E_g$ transition, frequently observed in octahedral nickel(II) complexes. For Ni^{II} in an octahedral field, the energies, *E*, of the states $^3T_{2g}$ and $^3A_{2g}$ relative to the spherical field are given by eqs 8 and 9.[22]

$$\text{For } {}^3T_{2g}: \quad E = -2Dq \tag{8}$$

$$\text{For } {}^3A_{2g}: \quad E = -12Dq \tag{9}$$

From eqs 8 and 9, it is seen that the energies of both $^3T_{2g}$ and $^3A_{2g}$ are linear functions of Dq. For any ligand or ligand combination that produces a spin-free octahedral nickel(II) complex, the difference in energy between the $^3T_{2g}$ state and the $^3A_{2g}$ state in the complex is 10Dq. Because the lowest-energy transition $^3A_{2g} \rightarrow {}^3T_{2g}$ is a direct measure of the energy difference of these states, Δ (or 10Dq) can be equated to the transition energy, i.e., the frequency of this band (cm^{-1}). Thus, in our case, 10Dq = 8695 cm^{-1}. This value is typical for octahedral nickel(II) complexes with predominantly O ligation.

Finally, the emission properties for all complexes were investigated in the solid state, but unfortunately no fluorescence was observed. This is most probably due to the quenching of the emissive organic ligand by the paramagnetic metal centers. In order to fully investigate and understand the emission properties of the complexes, the zinc analogues of the complexes should be synthesized and their optical properties investigated, and work is currently underway toward this goal.

■ CONCLUSIONS

In conclusion, the use of the new tripodal ligand 2-(β-naphthalideneamino)-2-(hydroxymethyl)-1-propanol) in cobalt, nickel, and copper chemistry has led to the synthesis of five new homometallic complexes, which were analyzed with regard to their magnetic, thermal, and optical properties. In

dx.doi.org/10.1021/ic301744e | *Inorg. Chem.* 2012, 51, 10461−10470

cobalt chemistry, we were able to isolate a mixed-valent pentanuclear complex that displays ferromagnetic interactions, while in nickel chemistry, we isolated mononuclear and tetranuclear ferromagnetic complexes. Finally, in copper chemistry, we isolated two tetranuclear clusters that can be considered as structural isomers. From our results so far, we are confident that this new ligand may lead to the synthesis of clusters with interesting structures and enhanced magnetic properties. Work is in progress to extend this body of work to heterometallic 3d−4f clusters, as a means of fully investigating the abilities of this new tripodal ligand for the synthesis of metallic clusters.

■ ASSOCIATED CONTENT

Ⓢ Supporting Information

Tables of bond distances and angles for **1**−**4** and structures for **4** and **5**. This material is available free of charge via the Internet at http://pubs.acs.org.

■ AUTHOR INFORMATION

Corresponding Author

*E-mail: komil@chemistry.uoc.gr.

Notes

The authors declare no competing financial interest.

■ ACKNOWLEDGMENTS

C.J.M. thanks The University of Crete (ELKE, Research Grant KA 3089) for funding.

■ REFERENCES

(1) Representative references and references cited therein: (a) Que, E. L.; Chang, C. *J Chem. Soc. Rev.* **2010**, *39*, 51. (b) Fricker, S. P. *Chem. Soc. Rev.* **2006**, *6*, 524. (c) Murray, L. J.; Dincă, M.; Long, J. R. *Chem. Soc. Rev.* **2009**, *38*, 1294. (d) Manoli, M.; Collins, A.; Parsons, S.; Candini, A.; Evangelisti, M.; Brechin, E. K. *J. Am. Chem. Soc.* **2008**, *130*, 11129. (e) Bogani, L.; Wernsdorfer, W. *Nat. Mater.* **2008**, *7*, 179.

(2) For example, see: (a) Karotsis, G.; Teat, S. J.; Wernsdorfer, W.; Piligkos, S.; Dalgarno, S. J.; Brechin, E. K. *Angew. Chem., Int. Ed.* **2009**, *48*, 8285. (b) Evangelisti, M.; Brechin, E. K. *Dalton Trans.* **2010**, *39*, 4672. (c) Manoli, M.; Collins, A.; Parsons, S.; Candini, A.; Evangelisti, M.; Brechin, E. K. *J. Am. Chem. Soc.* **2008**, *130*, 1112.

(3) (a) Milios, C. J.; Vinslava, A.; Wernsdorfer, W.; Moggach, S.; Parsons, S.; Perlepes, S. P.; Christou, G.; Brechin, E. K. *J. Am. Chem. Soc.* **2007**, *129*, 2754. (b) Rinehart, J. D.; Fang, M.; Evans, W. J.; Long, J. R. *Nat. Chem.* **2011**, *3*, 539.

(4) Brimblecombe, R.; Swiegers, G. F.; Dismukes, G. C.; Spiccia, L. *Angew. Chem., Int. Ed.* **2008**, *47*, 7335.

(5) For example, see: (a) Bünzli, J.-C. G.; Piguet, C. *Chem. Soc. Rev.* **2005**, *34*, 1048. (b) Kido, J.; Okamoto, Y. *Chem. Rev.* **2002**, *102*, 2357. (c) Stouwdam, J. W.; Hebbink, G. A.; Huskens, J.; Van Veggel, F. C. J. M. *Chem. Mater.* **2003**, *15*, 4604.6.

(6) Orfanoudaki, M.; Tamiolakis, I.; Siczek, M.; Lis, T.; Armatas, G. S.; Pergantis, S. A.; Milios, C. J. *Dalton Trans.* **2011**, *40*, 4793.

(7) Beedle, C. C.; Stephenson, C. J.; Heroux, K. J.; Wernsdorfer, W.; Hendrickson, D. N. *Inorg. Chem.* **2008**, *47*, 10798.

(8) Winpenny, R. E. P. *Dalton Trans.* **2002**, 1.

(9) Canaj, A. B.; Tzimopoulos, D.; Philippidis, A.; Kostakis, G. E.; Milios, C. J. *Inorg. Chem.* **2012**, *51*, 7451.

(10) (a) Rao, P. V.; Rao, C. P.; Wegelius, E. K.; Rissanen, K. *J. Chem. Crystallogr.* **2003**, *33*, 39. (b) Rao, C. P.; Sreedhara, A.; Rao, P. V.; Verghese, B. M.; Kolehmainen, E.; Lokanath, N. K.; Sridhar, M. A.; Prasad, J. S. *J. Chem. Soc., Dalton Trans.* **1998**, 2383.

(11) (a) Stocker, B.; Troester, M. A. *Inorg. Chem.* **1996**, *35*, 3154. (b) Muller, E.; Bernardinelli, G.; Reedijk, J. *Inorg. Chem.* **1995**, *34*, 5979. (c) Pullen, A. E.; Piotraschke, J.; Abboud, K. A.; Reynolds, J. R. *Inorg. Chem.* **1999**, *35*, 793. (d) Lhuachan, S.; Siripaisarnpipat, S.; Chaichit, N. *Eur. J. Inorg. Chem.* **2003**, 263.

(12) Kostakis, G. E.; Blatov, V. A.; Proserpio, D. M. *Dalton Trans.* **2012**, *41*, 4634.

(13) (a) Carlin, R. L. *Magnetochemistry*; Springer-Verlag: Berlin, 1986. (b) Kahn, O. *Molecular Magnetism*; Wiley-VCH: New York, 1993.

(14) Representative references and references cited therein: (a) Klöwer, F.; Lan, Y.; Nehrkorn, J.; Waldmann, O.; Anson, C. E.; Powell, A. K. *Chem.—Eur. J.* **2009**, *15*, 7413. (b) Yang, E. C.; Hendrickson, D. N.; Wernsdorfer, W.; Nakano, M.; Zakharov, L. N.; Sommer, R. D.; Rheingold, A. L.; Ledezma-Gairaud, M.; Christou, G. *J. Appl. Phys.* **2002**, *91*, 7382. (c) Zhang, Y.-Z.; Wernsdorfer, W.; Pan, F.; Wang, Z.-M.; Gao, S. *Chem. Commun.* **2006**, 3302. (d) Waldmann, O.; Ruben, M.; Ziener, U.; Müller, P.; Lehn, J. M. *Inorg. Chem.* **2006**, *45*, 6535. (e) Andres, H.; Clemente-Juan, J. M.; Aebersold, M.; Güdel, J. M.; Coronado, E.; Buettner, H.; Kearly, G.; Melero, J.; Burriel, R. *J. Am. Chem. Soc.* **1999**, *121*, 10028. (f) Palii, A. V.; Tsukerblat, B. S.; Coronado, E.; Clement-Juan, J. M.; Borras-Almenar, J. J. *Inorg. Chem.* **2003**, *42*, 2455. (g) Banci, L.; Bencini, A.; Benelli, C.; Gatteschi, D.; Zanchini, C. *Struct. Bonding (Berlin)* **1982**, *52*, 37. (h) Boča, R. *Struct. Bonding (Berlin)* **2006**, *117*, 1. (i) Moragues-Canovás, M.; Talbot-Eeckelaers, C. E.; Catala, L.; Lloret, F.; Wernsdorfer, W.; Brechin, E. K.; Mallah, T. *Inorg. Chem.* **2006**, *45*, 7038. (j) Clemente-Juan, J. M.; Coronado, E.; Gaita-Ariño, A.; Giménez-Saiz, C.; Güdel, H.-U.; Sieber, A.; Bircher, R.; Mutua, H. *Inorg. Chem.* **2005**, *44*, 3389. (k) Clemente-Juan, J. M.; Coronado, E.; Forment-Aliaga, A.; Galan-Mascaros, J. R.; Gimenez-Saiz, C.; Gomez-Garcia, C. J. *Inorg. Chem.* **2004**, *43*, 2689.

(15) Boeer, A. B.; Barra, A.-L.; Chibotaru, L. F.; Collison, D.; McInnes, E. J. L.; Mole, R. A.; Simeoni, G. G.; Timco, G. A.; Ungur, L.; Unruh, T.; Winpenny, R. E. P. *Angew. Chem., Int. Ed.* **2011**, *50*, 4007.

(16) (a) Borrás-Almenar, J. J.; Clemente-Juan, J. M.; Coronado, E.; Tsukerblat, B. S. *Inorg. Chem.* **1999**, *38*, 6081. (b) Borrás-Almenar, J. J.; Clemente-Juan, J. M.; Coronado, E.; Tsukerblat, B. S. *J. Comput. Chem.* **2001**, *22*, 985.

(17) For example, see: (a) Zhang, S.-Y; Chen, W.-Q.; Hu, B.; Chen, Y.-M.; Li, W.; Li, Y. *Inorg. Chem. Commun.* **2012**, *16*, 74. (b) Mukherjee, S.; Weyhermuller, T.; Bothe, E.; Wieghardt, K.; Chaudhuri, P. *Eur. J. Inorg. Chem.* **2003**, 863. (c) Paine, T. K.; Rentschler, E.; Weyhermuller, T.; Chaudhuri, P. *Eur. J. Inorg. Chem.* **2003**, 3167. (d) Aromi, G.; Bouwman, E.; Burzurí, E.; Carbonera, C.; Krzystek, J.; Luis, F.; Schlegel, C.; van Slageren, J.; Tanase, S.; Teat, S. J. *Chem.—Eur. J.* **2008**, *14*, 11158. (e) Moragues-Cánovas, M.; Helliwell, M.; Ricard, L.; Rivière, É.; Wernsdorfer, W.; Brechin, E. K.; Mallah, T. *Eur. J. Inorg. Chem.* **2004**, 2219. (f) Yang, E.-C.; Wernsdorfer, W.; Hill, S.; Edwards, R. S.; Nakano, M.; Maccagnano, S.; Zakharov, L. N.; Rheingold, A. L.; Christou, G.; Hendrickson, D. N. *Polyhedron* **2003**, *22*, 1727. (g) Halcrow, M. A.; Huffman, J. C.; Christou, G. *Angew. Chem., Int. Ed. Engl.* **1995**, *34*, 889. (h) Escuer, A.; Font-Bardía, M.; Kumar, S. B.; Solans, X.; Vicente, R. *Polyhedron* **1999**, *18*, 909. (i) Shiga, T.; Oshio, H. *Sci. Technol. Adv. Mater.* **2005**, *6*, 565. (j) Boskovic, C.; Rusanov, E.; Stoeckli-Evans, H.; Gudel, H. U. *Inorg. Chem. Commun.* **2002**, *5*, 881.

(18) Halcrow, M. A.; Sun, J.-S.; Huffman, J. C.; Christou, G. *Inorg. Chem.* **1995**, *34*, 4167.

(19) For example, see: (a) Castro, I.; Calatayud, M. L.; Lloret, F.; Sletten, J.; Julve, M. *J. Chem. Soc., Dalton Trans.* **2002**, 2397. (b) Haddad, M. S.; Wilson, S. R.; Hodgson, D. J.; Hendrickson, D. N. *J. Am. Chem. Soc.* **1981**, *103*, 384.

(20) (a) Halcrow, M. A.; Sun, J. S.; Huffman, J. C.; Christou, G. *Inorg. Chem.* **1995**, *34*, 4167. (b) Merz, L.; Haase, W. *J. Chem. Soc., Dalton Trans.* **1978**, 1595. (c) Merz, L.; Haase, W. *J. Chem. Soc., Dalton Trans.* **1980**, 875. (d) Mergehenn, R.; Merz, L.; Haase, W. *J. Chem. Soc., Dalton Trans.* **1980**, 1703. (e) Laurent, J.-P.; Bonnet, J.-J.; Nepveu, F.; Astheimer, H.; Walz, L.; Haase, W. *J. Chem. Soc., Dalton Trans.* **1982**, 2433. (f) Schwabe, L.; Haase, W. *J. Chem. Soc., Dalton Trans.* **1985**, 1909.

(21) (a) Lever, A. B. P. *Inorganic Electronic Spectroscopy*, 2nd ed.; Elsevier: Amsterdam, The Netherlands, 1984. (b) Galloway, K. W.; Whyte, A. M.; Wernsdorfer, W.; Sanchez-Benitez, J.; Kamenev, K. V.; Parkin, A.; Peacock, R. D.; Murrie, M. *Inorg. Chem.* **2008**, *47*, 7438. (c) Tiliakos, M.; Cordopatis, P.; Terzis, A.; Perlepes, S. P.; Manessi-Zoupa, E. *Polyhedron* **2001**, *20*, 2203. (d) Plakatouras, J. C.; Perlepes, S. P.; Mentzafos, D.; Terzis, A.; Bakas, T.; Papaefthymiou, V. *Polyhedron* **1992**, *11*, 2657. (e) Vakros, J.; Bourikas, K.; Perlepes, S.; Kordulis, C.; Lycourghiotis, A. *Langmuir* **2004**, *20*, 10542.
(22) Drago, R. S. *Physical Methods in Chemistry*; Saunders: Philadelphia, PA, 1977.